

# Arc-like magmas generated by mélange-peridotite interaction in the mantle wedge

E. A. Codillo<sup>1</sup>, V. Le Roux<sup>\*,2</sup>, H. R. Marschall<sup>3</sup>

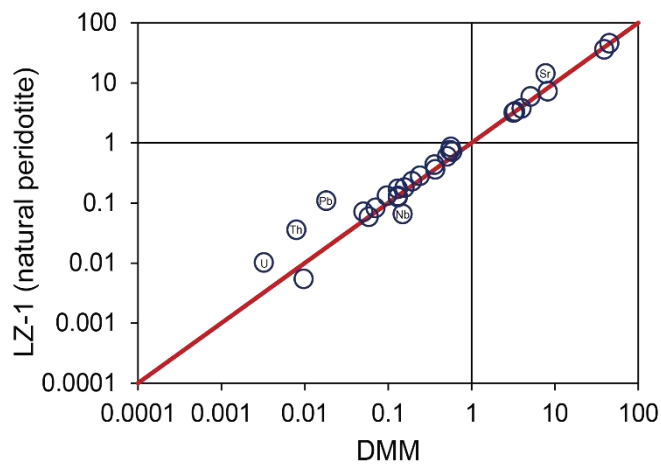
<sup>1</sup>Massachusetts Institute of Technology/Woods Hole Oceanographic Institution Joint Program in Oceanography/Applied Ocean Science and Engineering, Woods Hole, Massachusetts 02543, USA

<sup>2</sup>Department of Geology and Geophysics, Woods Hole Oceanographic Institution, 266 Woods Hole Road, Woods Hole Massachusetts 02543 USA

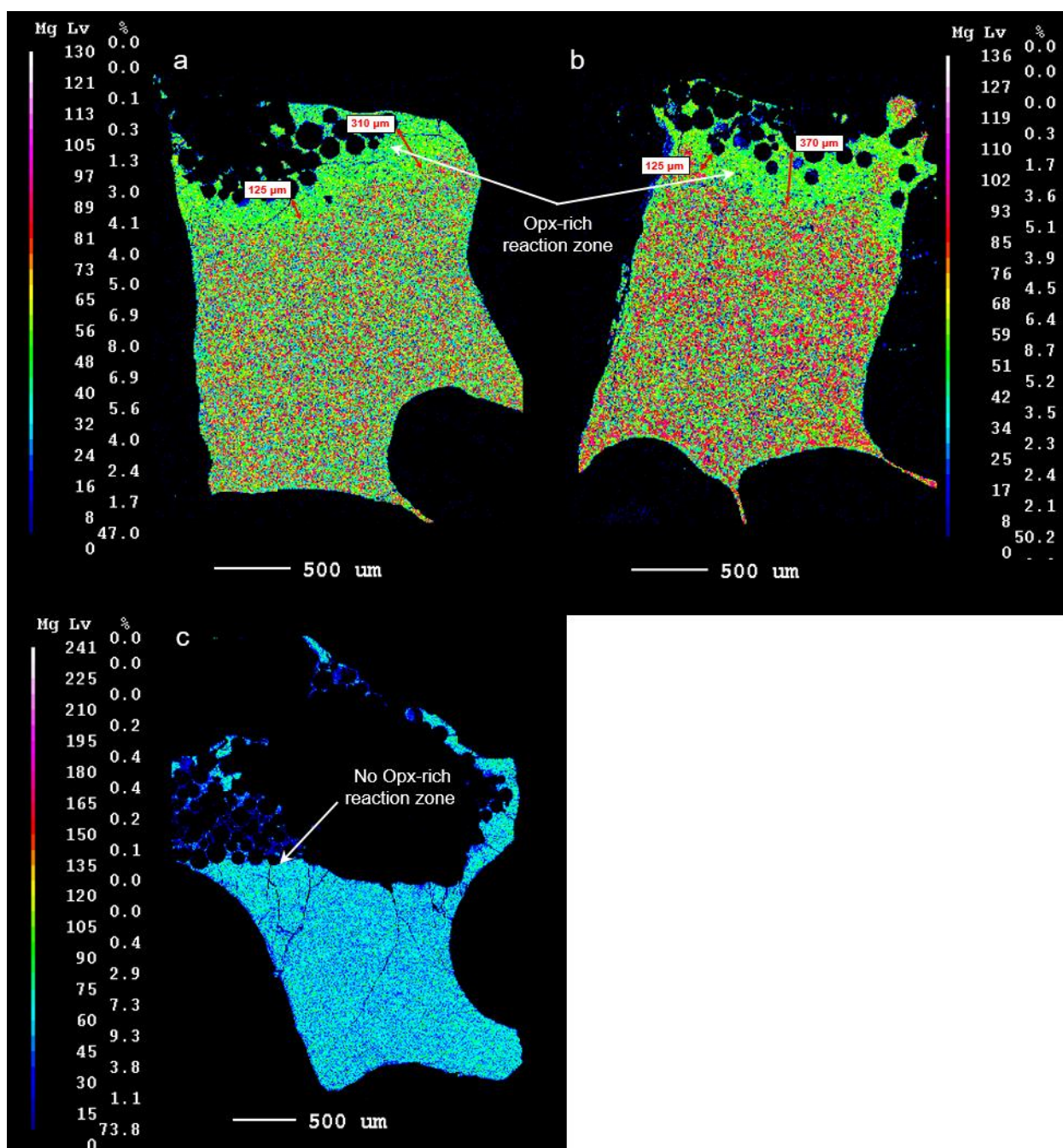
<sup>3</sup>Institut für Geowissenschaften, Goethe Universität Frankfurt, Altenhöferalle 1, 60438 Frankfurt am Main, Germany

\*corresponding author: vleroux@whoi.edu

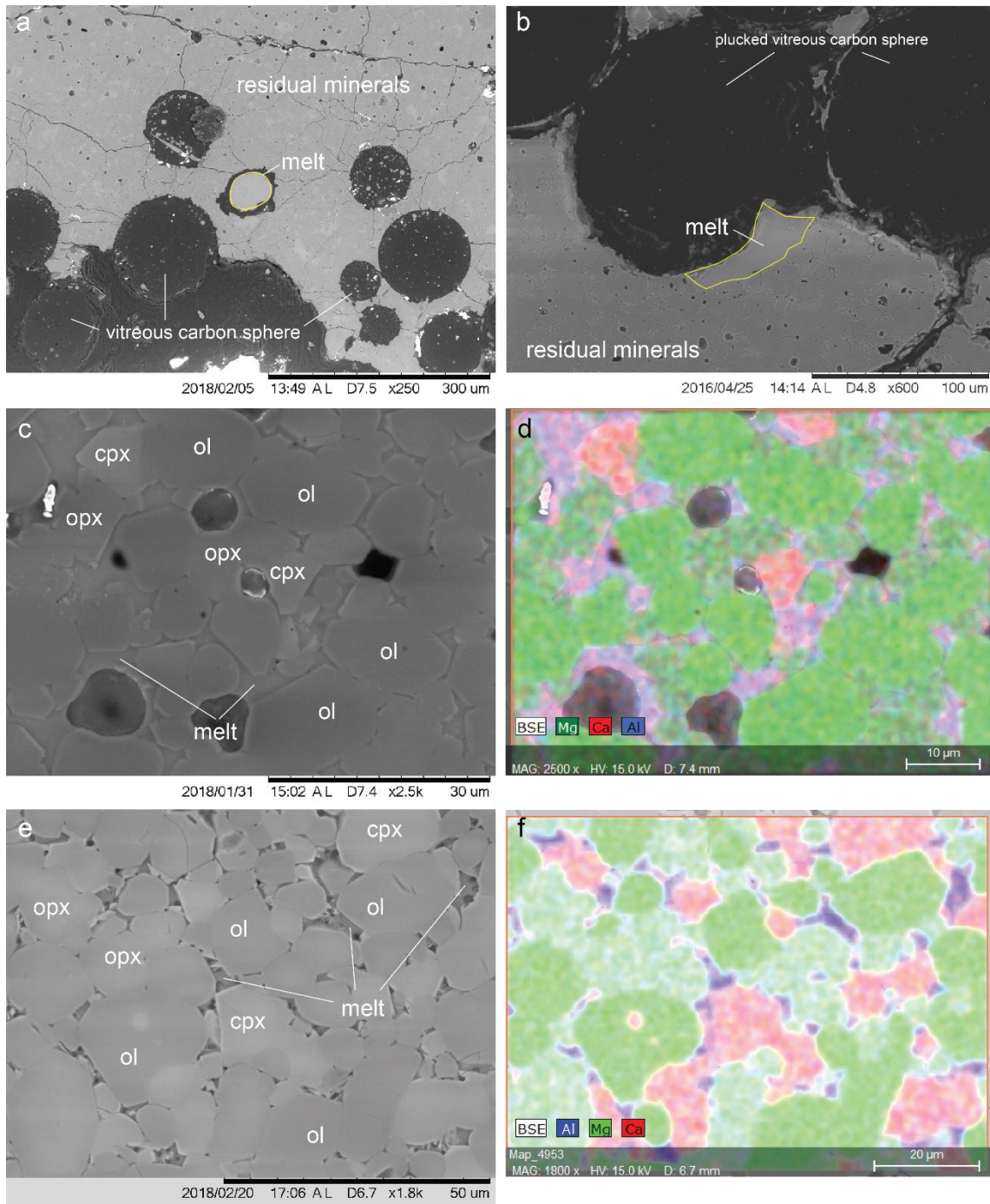
## Supplementary Figures



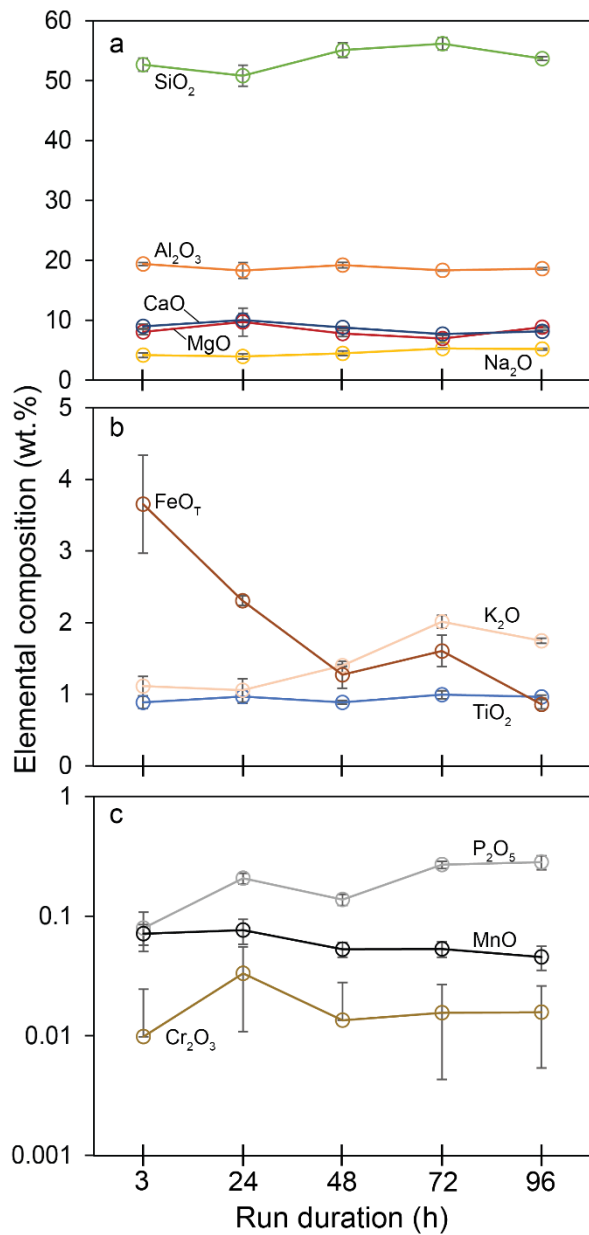
**Supplementary Figure 1 | Composition of natural peridotite LZ-1 used in this study, compared with DMM composition.** The plot demonstrates a close compositional similarity for major and trace elements between LZ-1 (Supplementary Dataset 1) and DMM<sup>1</sup> compositions. The red line is the 1:1 ratio line.



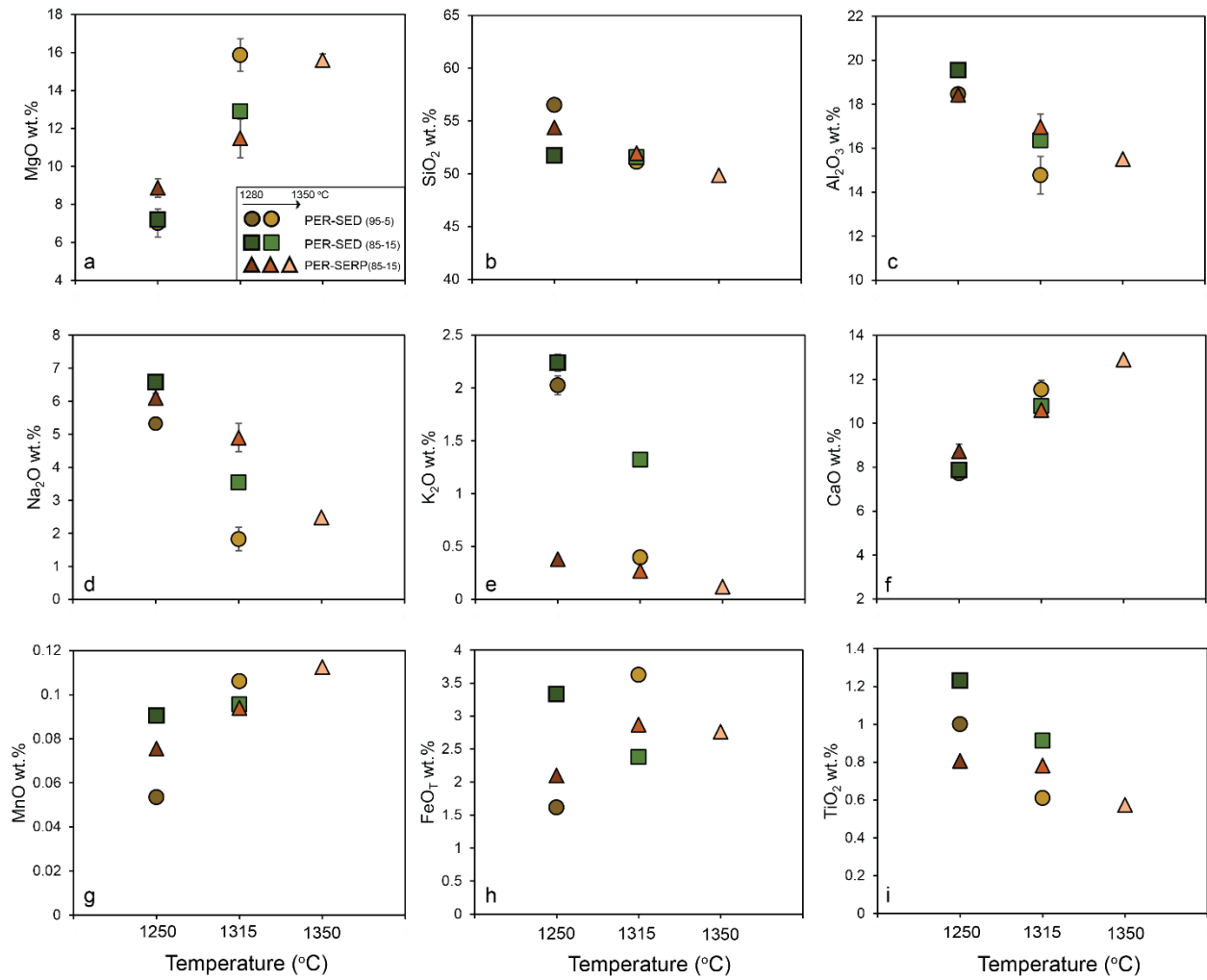
**Supplementary Figure 2 | Mg compositional maps of representative experiments.** Mg compositional maps of 72-h experiments performed at 1.5 GPa. (a) PER-SED (85-15) at 1280 °C and (b) PER-SED (85-15) at 1315 °C, showing a 125–370 μm-thick Opx-rich reaction zone (green areas). (c) No opx-rich reaction zone was observed in the 3-h experiment PER-SED (95-5) at 1.5 GPa and 1280 °C.



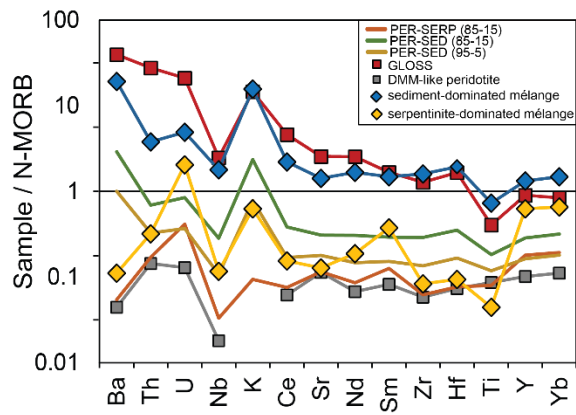
**Supplementary Figure 3 | Representative BSE and EDS images of experimental run products at 1.5 GPa.** Olivine (ol), Orthopyroxene (opx), Clinopyroxene (cpx) and melt are identified. Dark zones are holes/voids left by plucked out minerals during polishing. Dark round circles are polished (and sometimes plucked) vitreous carbon spheres. (a) A well-exposed circular melt pool occupying the outline of a carbon sphere in PER-SED 85-15 at 1315 °C, and (b) melt pool around a plucked carbon sphere in PER-SED 85-15 at 1280 °C. (c) BSE image and (d) Mg-Ca-Al chemical map of PER-SED 85-15 at 1280 °C highlighting the assemblage of ol + opx + cpx + melt. (e) BSE image and (f) Mg-Ca-Al chemical map of the near-solidus experiment PER-SERP 85-15 at 1230 °C highlighting the assemblage of ol + opx + cpx + minor amount of melt. Melt compositions from near-solidus experiments were not used in this study as abundant dendrites were noticed.



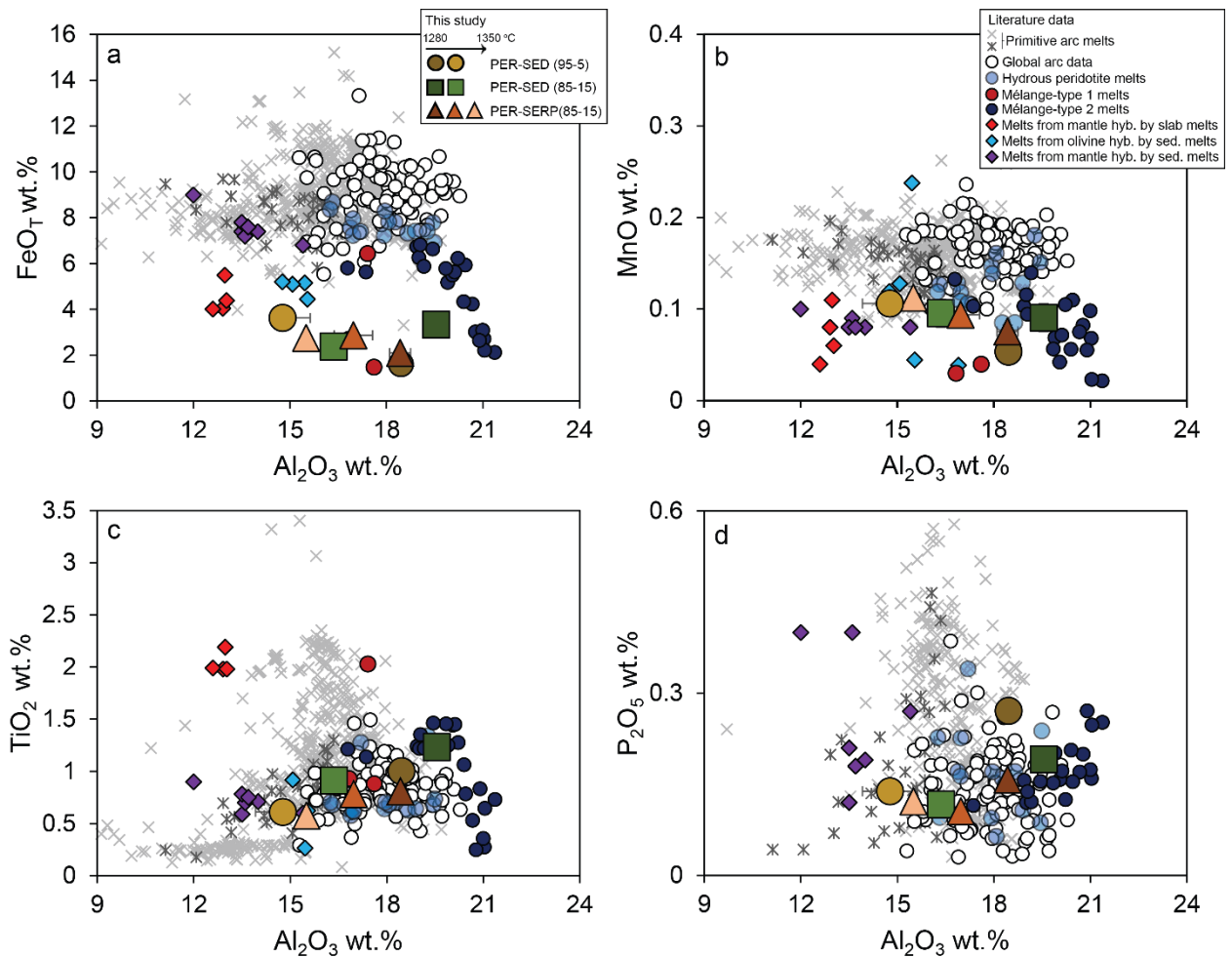
**Supplementary Figure 4 | Determination of minimum run duration through a time-series experiments.** Element compositional variations, (a) SiO<sub>2</sub>, Al<sub>2</sub>O<sub>3</sub>, CaO, MgO, Na<sub>2</sub>O, (b) FeO<sub>T</sub>, K<sub>2</sub>O, TiO<sub>2</sub>, (c) P<sub>2</sub>O<sub>5</sub>, MnO, Cr<sub>2</sub>O<sub>3</sub>, in a time series experiments at 1.5 GPa and 1280 °C (PER-SED 95-5; Supplementary Dataset 2), with run duration ranging from 3-h to 96-h. We chose a run duration of 72-h to ensure close approach to equilibrium. The data are plotted as averages with error bars representing 1 s.d.



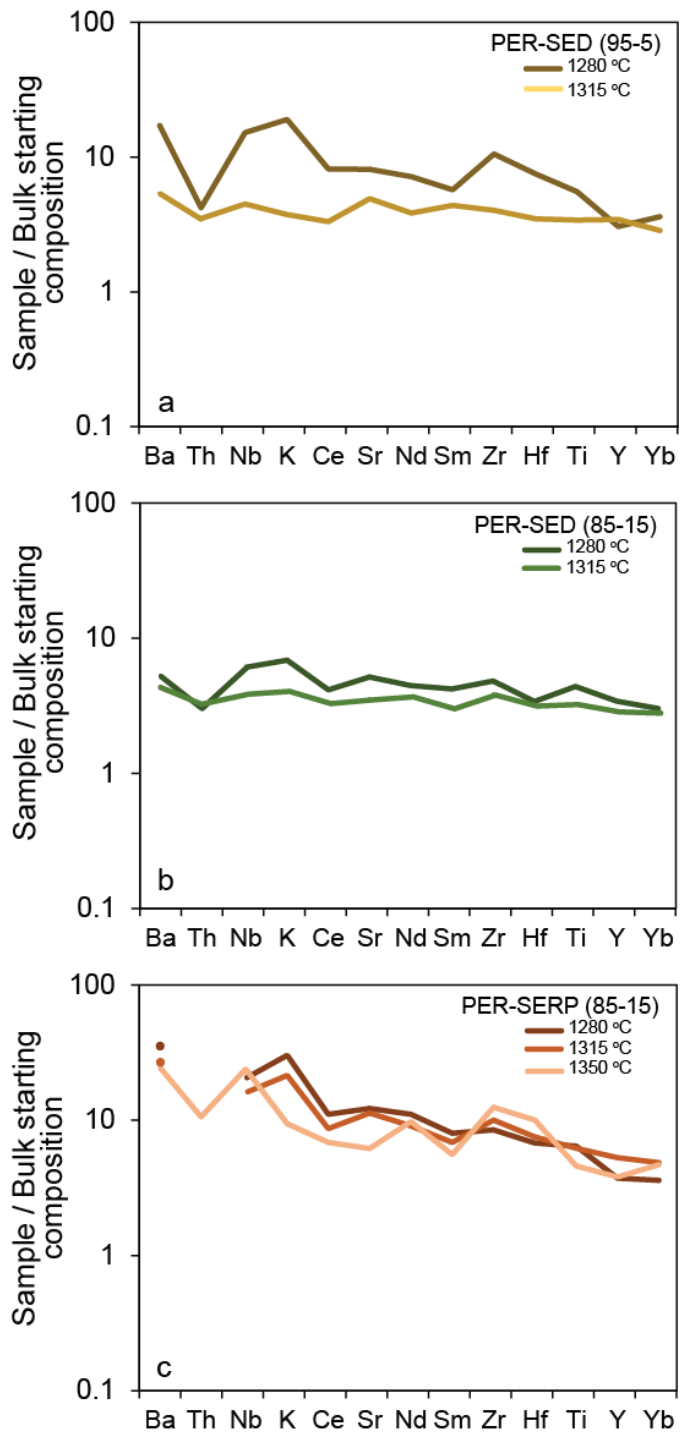
**Supplementary Figure 5 | Major element variations of experimental peridotite-mélange melts with temperature.** (a) MgO, (b) SiO<sub>2</sub>, (c) Al<sub>2</sub>O<sub>3</sub>, (d) Na<sub>2</sub>O, (e) K<sub>2</sub>O, (f) CaO, (g) MnO, (h) FeO<sub>T</sub>, (i) TiO<sub>2</sub> variations vs temperature (°C). The data are plotted as averages with error bars representing 1 s.d. (Supplementary Dataset 2).



**Supplementary Figure 6 | Trace element compositions of starting materials PER-SED and PER-SERP and their components.** DMM-like peridotite is LZ-1, sediment-dominated mélange is SY400B and serpentine-dominated mélange is SY325 (Supplementary Dataset 1). GLOSS composition is from Plank and Langmuir<sup>2</sup>. The average N-MORB value used in the normalization is from Gale *et al.*<sup>3</sup>

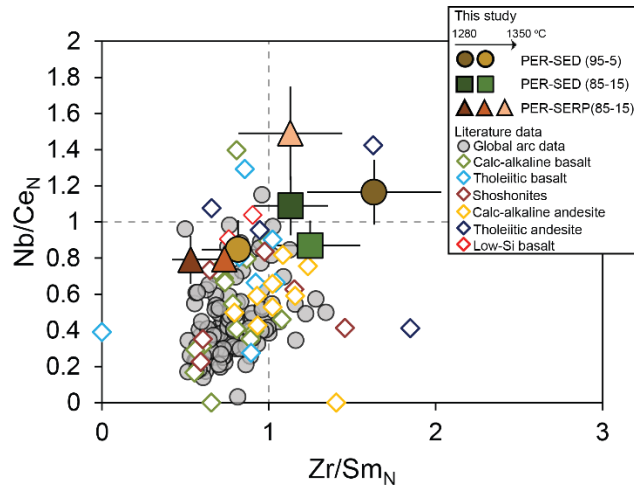


**Supplementary Figure 7 | Major element composition of experimental melts.** Major element variations (a)  $\text{FeO}_T$ , (b) MnO, (c)  $\text{TiO}_2$ , (d)  $\text{P}_2\text{O}_5$  vs  $\text{Al}_2\text{O}_3$  of experimental peridotite-mélange melts from this study compared to global arcs<sup>4</sup> (normalized to  $\text{MgO} = 6$  wt. %), two primitive arc melts compilations, and previous experimental studies<sup>5-7</sup>. The two primitive arc melts compilations are from Schmidt and Jagoutz<sup>8</sup> (gray asterisk) and Till *et al.*<sup>9</sup> (light gray cross). Hydrated peridotite melts are from Gaetani and Grove<sup>10</sup>. Experimental melts from mantle hybridized by slab melts and sediment melts are from Rapp *et al.*<sup>5</sup> and Mallik *et al.*<sup>7</sup>, respectively. Experimental melts of olivine hybridized by sediment melts are from Pirard and Hermann<sup>6</sup>. Experimental mélange-type 1 melts are from Castro and Gerya<sup>11</sup> and Castro *et al.*<sup>12</sup>, while the experimental mélange-type 2 melts are from Cruz-Uribe *et al.*<sup>13</sup> Our experiments are plotted as averages with error bars representing 1 s.d. All the data, including the literature, are plotted on volatile-free basis.

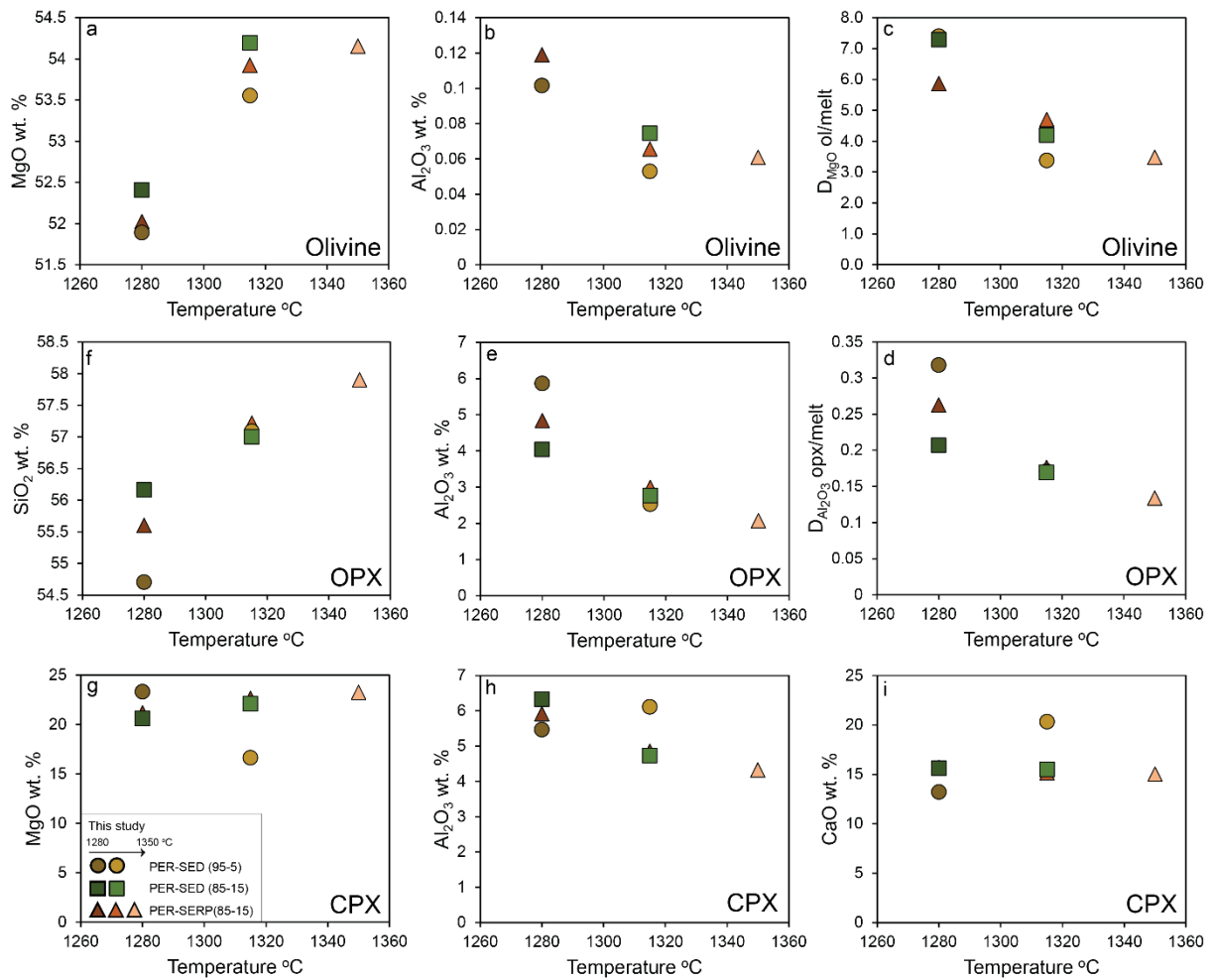


**Supplementary Figure 8 | Trace element compositions of experimental peridotite-mélange melts normalized to bulk starting compositions.** (a) PER-SED (95-5), (b) PER-SED (85-15) and (c) PER-SERP (85-15). The bulk starting compositions are summarized in Supplementary Dataset 1 and experimental melts compositions are reported in Supplementary Dataset 2.





**Supplementary Figure 9 | N-MORB normalized Nb/Ce versus Zr/Sm plot of experimental peridotite-mélange melts compared to arc magma compositions.** Arc magma literature databases include the global arc data<sup>4</sup> (circle symbol; normalized to MgO = 6 wt. %) and compiled primitive arc magmas<sup>8</sup> (diamond symbols). N-MORB value used in normalization is from Gale *et al.*<sup>3</sup>



**Supplementary Figure 10 | Major element and partition coefficient variations between minerals and melt with temperature.** Mineral chemistry data for olivine (ol), orthopyroxene (opx) and clinopyroxene (cpx) are summarized in Supplementary Dataset 5. The data are plotted as averages.

## Supplementary References

1. Workman, R. K. & Hart, S. R. Major and trace element composition of the depleted MORB mantle (DMM). *Earth Planet. Sci. Lett.* **231**, 53–72 (2005).
2. Plank, T. & Langmuir, C. H. The chemical composition of subducting sediment and its consequences for the crust and mantle. *Chem. Geol.* **145**, 325–394 (1998).
3. Gale, A., Dalton, C. A., Langmuir, C. H., Su, Y. & Schilling, J.-G. The mean composition of ocean ridge basalts. *Geochem. Geophys. Geosystems* **14**, 489–518 (2013).
4. Turner, S. J. & Langmuir, C. H. The global chemical systematics of arc front stratovolcanoes: Evaluating the role of crustal processes. *Earth Planet. Sci. Lett.* **422**, 182–193 (2015).
5. Rapp, R.P, Shimizu, N, Norman, M.D & Applegate, G.S. Reaction between slab-derived melts and peridotite in the mantle wedge: experimental constraints at 3.8 GPa. *Chem. Geol.* **160**, 335–356 (1999).
6. Pirard, C. & Hermann, J. Focused fluid transfer through the mantle above subduction zones. *Geology* **43**, 915–918 (2015).
7. Mallik, A., Nelson, J. & Dasgupta, R. Partial melting of fertile peridotite fluxed by hydrous rhyolitic melt at 2–3 GPa: implications for mantle wedge hybridization by sediment melt and generation of ultrapotassic magmas in convergent margins. *Contrib. Mineral. Petrol.* **169**, 48 (2015).
8. Schmidt, M. W. & Jagoutz, O. The global systematics of primitive arc melts. *Geochem. Geophys. Geosystems* **18**, 2817–2854 (2017).
9. Till, C. B. A review and update of mantle thermobarometry for primitive arc magmas. *Am. Mineral.* **102**, 931 (2017).
10. Gaetani, G. A. & Grove, T. L. The influence of water on melting of mantle peridotite. *Contrib. Mineral. Petrol.* **131**, 323–346 (1998).
11. Castro, A. & Gerya, T. V. Magmatic implications of mantle wedge plumes: Experimental study. *Lithos* **103**, 138–148 (2008).

12. Castro, A. *et al.* Melting Relations of MORB–Sediment Mélanges in Underplated Mantle Wedge Plumes; Implications for the Origin of Cordilleran-type Batholiths. *J. Petrol.* **51**, 1267–1295 (2010).
13. Cruz-Uribe, A. M., Marschall, H. R., Gaetani, G. A. & Le Roux, V. Generation of alkaline magmas in subduction zones by partial melting of mélange diapirs—An experimental study. *Geology* **46**, 343–346 (2018).